increasing degrees of polymerization up to DP = 10–12 and is thereafter essentially molecular weight independent. In contrast, the enthalpy change associated with liquid crystalline phase transitions is molecular weight independent. The dynamics of mesophase formation, including the rate of decrease of the number of disclinations per unit volume and the rate of increase of the size of the nematic "domain", is strongly molecular weight dependent. Both rates decrease with increasing polymer molecular weight.

**Acknowledgment.** Financial support of this work by the Office of Naval Research and by the Army Research Office is gratefully acknowledged.

**Registry No.** M, 120411-48-5; D, 120411-49-6; 4-6-PMA, 120416-97-9.

## References and Notes

(1) Frosini, A.; Levita, G.; Lupinacci, D.; Magagnini, P. L. *Mol. Cryst. Liq. Cryst.* **1981**, *66*, 21.
(2) Kostromin, S. G.; Talroze, R. V.; Shibaev, V. P.; Plate, N. A. *Makromol. Chem., Rapid Commun.* **1982**, *3*, 803.
(3) Portugall, M.; Ringsdorf, H.; Zentel, R. *Makromol. Chem.* **1982**, *183*, 2311.
(4) Stevens, H.; Rehage, G.; Finkelmann, H. *Macromolecules* **1984**, *17*, 851.
(5) Uchida, S.; Morita, K.; Miyoshi, K.; Hashimoto, K.; Kawasaki, K. *Mol. Cryst. Liq. Cryst.* **1988**, *155*, 93.
(6) Shibaev, V. *Mol. Cryst. Liq. Cryst.* **1988**, *155*, 189.
(7) Percec, V.; Hahn, B. *Macromolecules*, in press.
(8) Percec, V.; Pugh, C. In *Side Chain Liquid Crystalline Polymers*; McArdle, C. B., Ed.; Blackie: Glasgow, 1989; p 30.
(9) Finkelmann, H., private communication.
(10) Demus, D.; Richter, L. *Texture of Liquid Crystals*; Verlag Chemie: Weinheim, 1978.
(11) Gray, G. W.; Goodby, J. W. *Smectic Liquid Crystals. Textures and Structures*; Leonard Hill: Glasgow, 1984.
(12) Percec, V.; Tomazos, D. *J. Polym. Sci., Part A: Polym. Chem.* **1989**, *27*, 999.
(13) Sogah, D. Y.; Hertler, W. R.; Webster, O. W.; Cohen, G. M. *Macromolecules* **1987**, *20*, 1473.
(14) Pugh, C.; Percec, V. *Polym. Prepr. (Am. Chem. Soc., Div. Polym. Chem.)* **1985**, *26*(2), 303.
(15) Kreuder, W.; Webster, O. W.; Ringsdorf, H. *Makromol. Chem., Rapid Commun.* **1986**, *7*, 5.
(16) Percec, V.; Hsu, C. S.; Tomazos, D. *J. Polym. Sci., Polym. Chem. Ed.* **1988**, *26*, 2047.
(17) Percec, V.; Hahn, B. *J. Polym. Sci., Part A: Polym. Chem.*, in press.
(18) Percec, V.; Tomazos, D. *Macromolecules* **1989**, *22*, 1512.
(19) Geib, H.; Hisgen, B.; Pschorn, U.; Ringsdorf, H.; Spiess, H. W. *J. Am. Chem. Soc.* **1982**, *104*, 917.
(20) Spiess, H. W. *Pure Appl. Chem.* **1985**, *57*, 1617.
(21) Boeffel, C.; Spiess, H. W.; Hisgen, B.; Ringsdorf, H.; Ohm, H.; Kirste, R. G. *Makromol. Chem., Rapid Commun.* **1986**, *7*, 777.
(22) Boeffel, C.; Hisgen, B.; Pschorn, U.; Ringsdorf, H.; Spiess, H. W. *Isr. J. Chem.* **1983**, *23*, 388.
(23) Engel, M.; Hisgen, B.; Keller, R.; Kreuder, W.; Reck, B.; Ringsdorf, H.; Schmidt, H. W.; Tschirner, P. *Pure Appl. Chem.* **1985**, *57*, 1009.
(24) Wassmer, K. H.; Ohmes, E.; Portugall, M.; Ringsdorf, H.; Kothe, G. *J. Am. Chem. Soc.* **1985**, *107*, 1511.
(25) Percec, V.; Pugh, C. Oligomers. In *Encyclopedia of Polymer Science and Engineering*, 2nd ed.; Mark, H. F.; Bikales, N. M.; Overberger, C. G.; Menges, G., Eds.; Wiley: New York, 1987; Vol. 10, p 432.
(26) Kohne, B.; Praefcke, K.; Ringsdorf, H.; Tschirner, P. *Liq. Cryst.* **1989**, *4*, 165.
(27) Blumstein, A. *Polym. J. (Tokyo)* **1985**, *17*, 277.
(28) Percec, V.; Nava, H.; Jonsson, H. *J. Polym. Sci., Part A: Polym. Chem.* **1987**, *25*, 1943.
(29) Percec, V.; Nava, H. *J. Polym. Sci., Part A: Polym. Chem.* **1987**, *25*, 405.
(30) Frank, C. F. *Discuss. Faraday Soc.* **1958**, *25*, 19.
(31) Shiwaku, T.; Nakai, H.; Hasegawa, H.; Hashimoto, H. *Polym. Commun.* **1987**, *28*, 174.
(32) Feijoo, J. L.; Ungar, G.; Owen, A. J.; Keller, A.; Percec, V. *Mol. Cryst. Liq. Cryst.* **1988**, *155*, 487.
(33) Rojstaezer, S.; Stein, R. S. *Mol. Cryst. Liq. Cryst.* **1988**, *157*, 487.
(34) Illers, K. H. *Eur. Polym. J.* **1974**, *10*, 911.
(35) Hessel, F.; Herr, R. P.; Finkelmann, H. *Makromol. Chem.* **1987**, *188*, 1597.
(36) Ratna, B. R.; Chandrasekhar, S. *Mol. Cryst. Liq. Cryst.* **1988**, *162B*, 157.
(37) Richardson, M. J. In *Comprehensive Polymer Science*; Sir Allen, G., Ed.; Pergamon Press: Oxford, New York, 1989; Vol. 1, p 867.
(38) Mandelkern, L. In *Comprehensive Polymer Science*; Sir Allen, G., Ed.; Pergamon Press: Oxford, New York, 1989; Vol. 2, p 363.

# Detailed Structural Analysis of Polysiloxane Antifoam Agents Using Carbon-13 and Silicon-29 NMR Spectroscopy

**I. R. Herbert and A. D. H. Clague***

*Shell Research Ltd., Thornton Research Centre, P.O. Box 1, Chester CH1 3SH, England.*
*Received July 25, 1988*

ABSTRACT: Polysiloxane (silicone) antifoam agents are commonly used in the oil industry to reduce or prevent foam formation in nonaqueous systems. In order to improve the understanding of the mechanism of antifoam action, detailed structural analysis of a range of commercially available antifoam agents has been performed by carbon-13 and silicon-29 NMR spectroscopy. Two types of polysiloxanes have been encountered: homopolymers containing methyl(trifluoropropyl)siloxane units and copolymers containing both methyl(trifluoropropyl)- and dimethylsiloxane units. Particular emphasis has been placed on quantitative NMR methods and microstructural analysis of the copolymers.

## 1. Introduction

The efficiency of processes such as gas/liquid separation can be greatly impaired by unwanted foam or froth formation. Polysiloxane (silicone) antifoam agents are commonly used to reduce or prevent foam formation in nonaqueous systems such as those found in oil production and processing. As part of the study, a range of commercial polysiloxanes were characterized by nuclear magnetic resonance (NMR) spectroscopy to provide a better understanding of the links between molecular structure and performance of antifoam agents. This report describes silicon-29 and carbon-13 NMR methods that have been used to perform detailed structural analysis of typical polysiloxane antifoam agents.

The silicon-containing antifoam agents normally encountered are linear polysiloxanes having the general

0024-9297/89/2222-3267$01.50/0 

formula where $n$ can range through several orders of

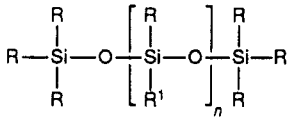

magnitude. For all samples studied here, R = $CH_3$ and $R^1$ = $CH_3$ or $CH_2CH_2CF_3$. Throughout this report a commonly adopted shorthand will be used to describe polysiloxane structures:[1] end-chain units $(CH_3)_3SiO_{1/2}$ are denoted by the letter M, whereas midchain units $O_{1/2}Si(CH_3)_2O_{1/2}$ and $O_{1/2}Si(CH_3)(CH_2CH_2CF_3)O_{1/2}$ are denoted by D and $D^1$, respectively. Only two types of polymers have been encountered in this study, namely, homopolymers of the form $MD^1{}_nM$, and (random) copolymers of the type $MD_nD^1{}_mM$.

Silicon-29 NMR spectroscopy is well suited to the study of polysiloxanes.[1-4] Silicon–29 is a spin-$^1/_2$ nucleus (hence it gives sharp resonances) and it also has a relatively high NMR receptivity (approximately twice that of carbon-13). In addition, it exhibits a reasonably large chemical shift range such that signals due to M- and D-type polysiloxane units are well separated. Furthermore, resonances due to D and $D^1$ are also readily distinguished on the basis of chemical shift.

Carbon-13 NMR spectroscopy provides complementary information since it enables identification of the various R groups present in polysiloxanes.

The present work describes silicon-29 and carbon-13 NMR measurements on a variety of commercial polysiloxanes. Particular emphasis is placed on the conditions necessary to obtain quantitative silicon-29 spectra such that an accurate determination of polysiloxane composition can be obtained.

## 2. Experimental Section

Two types of commercially available antifoam agent were studied: type A, which are homopolymers, and type B, which are copolymers. Carbon-13 and silicon-29 NMR measurements were performed on a Bruker MSL 300 NMR spectrometer (operating field, 7 T) using a Bruker 10 mm VSP solution-state probe. Samples were contained in 10-mm-o.d. NMR tubes as approximately 65% w/w solutions in acetone-$d_6$ (sample volume was approximately 2.5 mL). Unless otherwise stated, 10 mg of the relaxation reagent $Fe(acac)_3$ was added to each sample.

Quantitative silicon-29 NMR measurements were performed with inverse-gated broadband proton decoupling, a magnetization tip angle of about 45° (5 μs), and a relaxation delay of 12 s. The typical spectral width was 18000 Hz, which, with a Fourier-transformed data size of 32K points, gave a digital resolution of about 1.1 Hz. Silicon-29 chemical shifts were referenced to external tetramethylsilane.

Silicon-29 spin–lattice relaxation time measurements were performed by the inversion recovery method with a relaxation delay of 20 s and $\tau$ values ranging from 0.1 to 20 s.

Quantitative carbon-13 measurements were performed with inverse-gated proton decoupling, a magnetization tip angle of 45° (4.9 μs), and a relaxation delay of 5 s. The spectral width was generally chosen as 18000 Hz, with a transformed data size of 32K points, giving a digital resolution of about 1.1 Hz. Chemical shifts were referenced to TMS via the central resonance of internal acetone-$d_6$ taken as 29.8 ppm.

## 3. Results and Discussion

**3.1. Quantitative Silicon-29 NMR Measurements.** There are two factors which have an important bearing on the ability to perform quantitative silicon-29 NMR measurements.[1]

First, $^{29}Si$ tends to have a relatively long spin–lattice relaxation time ($T_1$). Generally, in order to achieve an adequate signal-to-noise ratio for $^{29}Si$, the sequence (pulse–acquire data) has to be repeated several hundreds or thousands of times. One requirement for quantitative results is that the delay between successive radiofrequency pulses is at least $5T_1$. Hence, very long measurement times may be required for samples which have a long $^{29}Si$ $T_1$. This problem can be overcome by the addition of a shiftless relaxation reagent such as $Fe(acac)_3$ to the sample, which leads to a significant reduction in $T_1$, and hence overall measurement times. From a series of inversion recovery experiments performed on a sample of the polysiloxane A1 containing 10 mg of $Fe(acac)_3$ (see Figure 1), we have established that the $T_1$ relaxation times for the various silicon environments present all fall close to 2 s. Thus we are satisfied that the conditions we have chosen for silicon-29 observation (45° pulse, 12-s relaxation delay) lead to quantitatively reliable results.

The second factor affecting quantitation relates to the fact that silicon-29 possesses a negative magnetogyric ratio. In the presence of complete proton decoupling the nuclear Overhauser enhancement (NOE) for silicon can range from 0 to −2.52, depending on the relaxation mechanism. Thus, signal intensities can range from +1 to −1.52, and in certain cases very weak or "null" signals can occur. This is amply demonstrated in Figure 2a,b which shows $^{29}Si$ spectra of sample A1 [no added $Fe(acac)_3$]. Figure 2a was obtained with inverse gated decoupling (i.e., the decoupler is only on during data acquisition) which "quenches" any NOE effects. Figure 2b was obtained with nongated decoupling and shows that the NOE for the silicon nucleus resonating at ca. 10 ppm is close to −1 (note all signals have been given an arbitrarily positive phase). Figure 2c, which was also obtained in the presence of full proton decoupling, indicates that NOE effects can also be quenched by addition of $Fe(acac)_3$. In practice, the combination of inverse gated decoupling and addition of $Fe(acac)_3$ is used to remove NOE effects.

To summarize, to ensure that our silicon-29 NMR measurements are quantitatively reliable we have (i) used inverse gated decoupling and $Fe(acac)_3$ to suppress NOE effects and (ii) taken due account of silicon-29 $T_1$ relaxation times in the presence of $Fe(acac)_3$ in selecting a suitable relaxation delay.

**3.2. Characterization of the Polysiloxane Series A.** NMR analysis of this family of polysiloxanes is relatively straightforward. Silicon-29 NMR spectra for the three samples, A1, A2, and A3, are shown in Figure 3.

Starting with sample A1, the simplicity of its spectrum indicates that the sample is a homopolymer (i.e., the same siloxane repeat unit occurs throughout). The resonance at ca. 9 ppm occurs in the region associated with end-chain siloxane units of the form $R_3SiO_{1/2}$. The remaining resonances, which all lie around −22.5 ppm, are indicative of chain siloxane units, $O_{1/2}SiR_2O_{1/2}$. It then follows from intensity considerations that the two resonances at lowest frequency are due to the second and third (and last-but-one and last-but-two) siloxane units in the chain, while the most intense resonance is due to those siloxane units further along the chain. (The environments of the second and third silicons are sufficiently distinct from those further along the chain to give separate resonances.) Integration of signal intensities due to end-chain silicon and chain silicon enables the calculation of the *average* chain length of the polymer. For A1 an *average* composition $MD^1{}_{16.5}M$ was determined.

The spectra of the A2 and A3 both show a similar set of resonances to A1, indicating that they have the same general structure. A lowering of the relative intensities of signals due to the first three siloxane units in going from A1 through A2 to A3 is in keeping with an increase in chain

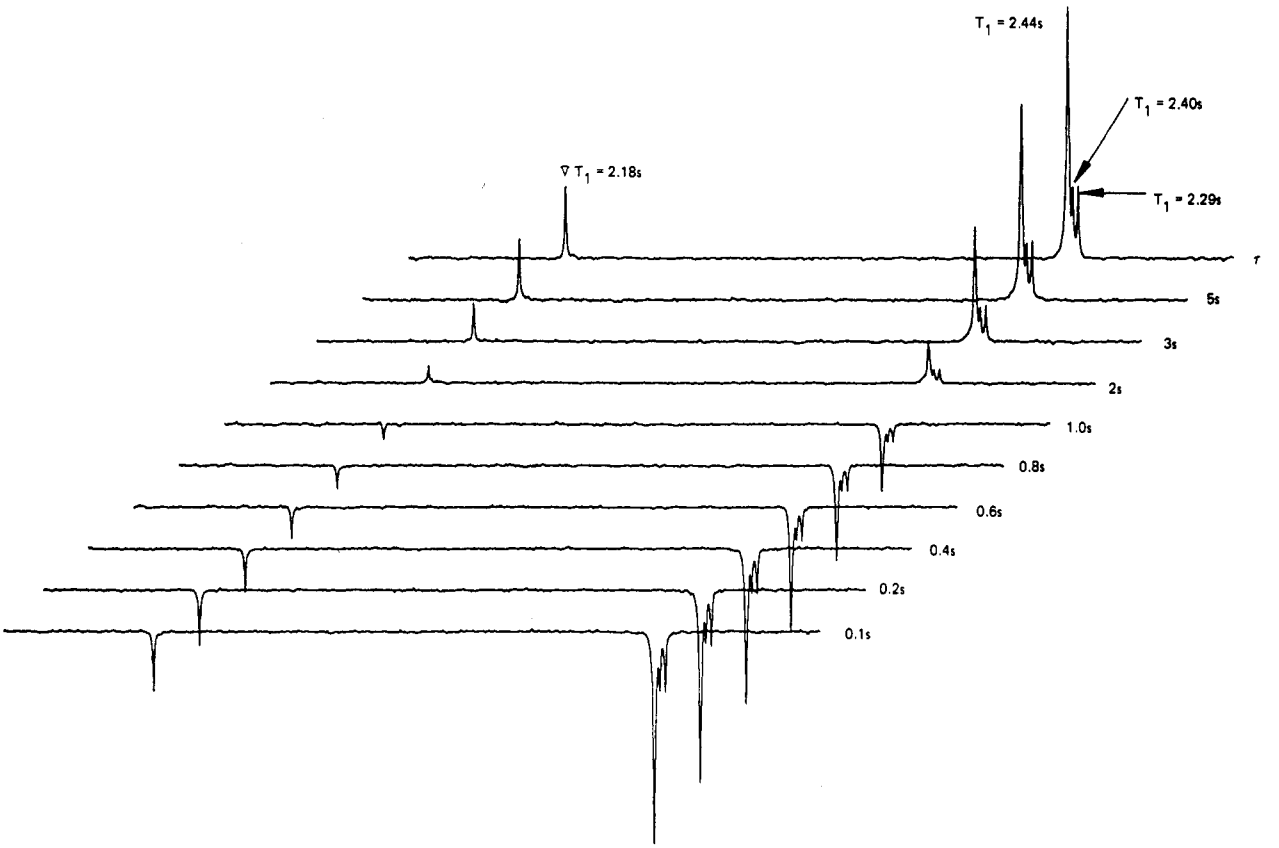


**Figure 1.** Series of $^{29}Si$ inversion recovery experiments [180°–$\tau$–acquire] performed on A1 containing 4 mg/mL $Fe(acac)_3$.

length. Average chain compositions for A2 and A3 were calculated as $MD^1_{25.5}M$ and $MD^1_{60.7}M$, respectively. The somewhat broader lines observed for A3 can be readily ascribed to a reduction in silicon molecular mobility as a result of the relatively high molecular weight of this sample.

Identification of the alkyl groups present in this family of polysiloxanes comes from carbon-13 NMR analysis. The carbon-13 spectrum of A1 is shown in Figures 4 and 5. The assignments indicated were aided by the following: (i) Chemical shifts are taken into consideration. (ii) Resonances due to silicon-bonded carbon show silicon-29 satellites [as silicon-29 is only 4.6% abundant, 95.4% of the signal intensity due to silicon-bonded carbon occurs as a singlet, while the remainder appears as a doublet with splitting $J(^{13}C^{29}Si)$]. (iii) Resonances due to the $\beta$ and $\gamma$ carbons in the $CH_2CH_2CF_3$ substituent appear as 1:3:3:1 quartets as a result of spin–spin coupling to three equivalent fluorine-19 nuclei ($^{19}F$, spin $^1/_2$, 100% natural abundance).

Since it is known from the silicon-29 measurements that the sample is a homopolymer, it follows from the signal intensities observed in the carbon-13 spectrum that the polysiloxane repeat unit $D^1$ is $O_{1/2}SiMe(CH_2CH_2CF_3)O_{1/2}$. The second weaker methyl resonance observed (1.8 ppm) is therefore readily assigned to the end-chain unit M = $Me_3SiO_{1/2}$. Ratios of integrated intensities of the signals due to the three types of alkyl substituents lead to a value of average polymer chain length that is in close agreement with that obtained from silicon-29 measurements. To conclude, the structure of the polymer is now fully characterized by NMR spectroscopy.

Samples A2 and A3 show similar $^{13}C$ NMR spectra except that the relative intensity of the resonance due to end-chain methyl is reduced as the polymer molecular weight increases. Detailed analytical data for this family of polymers is given in Table I.

**Table I**
**NMR Parameters and Related Analytical Data for the Polysiloxane Series A1–A3**

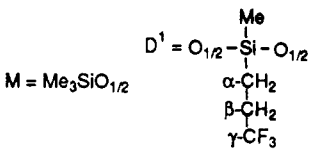


| sample | av chain comp | av molec wt |
|---|---|---|
| A1 | $MD^1_{16.5}M$ | 2739 |
| A2 | $MD^1_{25.5}M$ | 4145 |
| A3 | $MD^1_{60.7}M$ | 9643 |

| $^{29}Si$ chem shifts | | $^{13}C$ chem shifts | |
|---|---|---|---|
| $MD^1_1D^1_2D^1_n$ | $\delta(^{29}Si)$/ppm | | $\delta(^{13}C)$/ppm |
| M | 9.3 | M = Me | 1.8 |
| $D^1_1$ | −22.9 | $D^1$ = | |
| $D^1_2$ | −22.5 | Me | −0.6 |
| $D^1_n$ | −22.2 | α-$CH_2$ | 9.9 |
| | | β-$CH_2$ | 28.6 |
| | | γ-$CF_3$ | 128.9 |

**3.3. Characterization of Antifoam Agent B1. 3.3.1. General Structural Analysis.** In contrast to the A series of polymers, the silicon-29 spectrum of B1 (see Figure 6) shows a complex set of resonances due to siloxane chain units and is in keeping with a (random) copolymer species.

Interestingly, however, no resonances are observed in the region associated with end-chain silicon (5–15 ppm, not illustrated). A complementary gel-permeation chromatography study has revealed that this sample has a very high molecular weight (number-average MW ca. 54 000), which therefore explains our failure to observe these signals.

Prior to any detailed analysis of the silicon-29 spectrum, it is necessary to discuss the carbon-13 NMR results for B1. The carbon-13 spectrum of B1 (not illustrated) com-

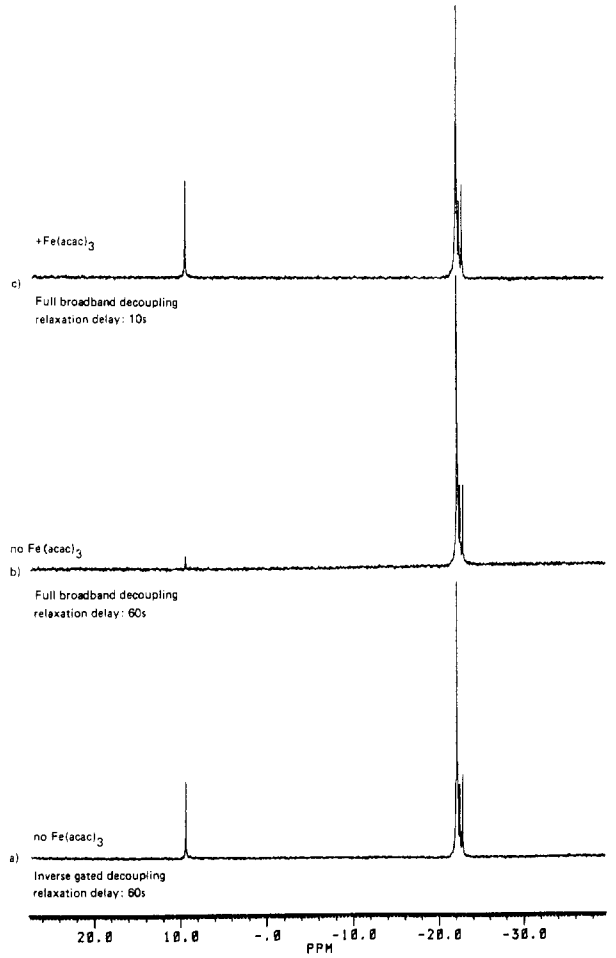


**Figure 2.** $^{29}Si$ NMR spectra of the polysiloxane A1, demonstrating the effects of inverse gated decoupling and $Fe(acac)_3$.

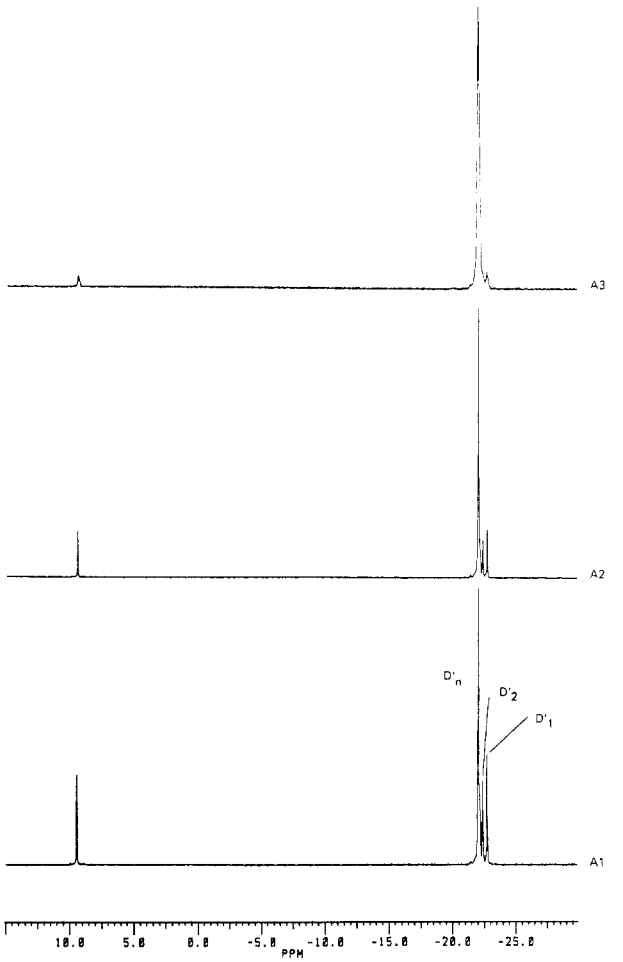


**Figure 3.** $^{29}Si$ NMR spectra of the A series of polysiloxanes $MD^1_nM$.

prises resonances due to three types of siloxane substituent. Two of these are readily identified as the methyl and trifluoropropyl groups in a $D^1 = O_{1/2}SiMe(CH_2CH_2CF_3)O_{1/2}$ unit (cf. A-type samples). The remaining substituent type is methyl and is therefore assigned to the chain unit $D = O_{1/2}Si(Me)_2O_{1/2}$. From ratios of integrated signal intensity, we have calculated the abundances of D and $D^1$ units as approximately 60% and 40%, respectively. In addition to these polysiloxane carbon resonances, the carbon-13 NMR spectrum also shows a signal due to two cosolvent components: one is readily identified as diisobutyl ketone; the second also appears to be a $C_9$ ketone, but its identity has so far eluded us.

**3.3.2. Detailed Structural Analysis of Polymer Microstructure.** Having established the identities of the two types of polymer chain unit in B1, we can now return to the analysis of the $^{29}Si$ NMR spectrum (Figure 6), which will lead to a detailed description of the polymer microstructure. The spectrum can be conveniently divided into two regions: signals from −19.0 to −22.0 ppm are assigned to D-type units, while signals from −22.0 to −24.5 ppm are assigned to $D^1$-type units. There are two factors that enable us to make this decision: first, we know the abundances of D and $D^1$ from the $^{13}C$ measurements; second, the $D^1$ units in the A samples resonate in the lower frequency region.

Each region can be further divided into three sets of resonances. In general, silicon chemical shifts are sensitive to the nature of neighboring siloxane groups. Thus, for example, the central $D^1$ unit in a $D^1D^1D^1$ triad grouping can be expected to resonate at a different frequency from the central $D^1$ unit in a $DD^1D$ triad grouping. Taking all

**Table II**
**Silicon-29 Chemical Shifts and Observed Triad Abundances for the Polysiloxane Antifoam Agent B1**

| triad[a] | $\delta(^{29}Si)$/ppm | % abundance |
|---|---|---|
| D centered | | |
| DDD | −21.6 | 22.5 |
| $DDD^1 + D^1DD$ | −20.8 | 30.8 |
| $D^1DD^1$ | −20.1 | 10.2 |
| total | | 63.5 |
| $D^1$ centered | | |
| $DD^1D$ | −24.0 | 16.3 |
| $DD^1D^1 + D^1D^1D^1$ | −23.1 | 16.2 |
| $D^1D^1D^1$ | −22.4 | 4.0 |
| total | | 36.5/100.0 |

[a] $D = O_{1/2}SiMe_2O_{1/2}$; $D^1 = O_{1/2}SiMe(CH_2CH_2CF_3)O_{1/2}$.

possible combinations, there are six different triad groupings, three D-centered triads and three $D^1$-centered triads:

| D-centered triads | $D^1$-centered triads |
|---|---|
| DDD | $DD^1D$ |
| $DDD^1/D^1DD$ | $DD^1D^1/D^1D^1D$ |
| $D^1DD$ | $D^1D^1D^1$ |

(note the equivalances of $DDD^1$ and $D^1DD$ and similarly $DD^1D^1$ and $D^1D^1D$). Assignments of the various triad resonances are indicated in Figure 6, and were made on the basis that (a) the approximate shift of the $D^1D^1D^1$ triad is already known from our study of the A-type samples and (b) there is a degree of regularity in chemical shift change in going, for example, from $D^1D^1D^1$ to $DD^1D$. Approximate chemical shifts and observed abundances for the six triads are given in Table II.

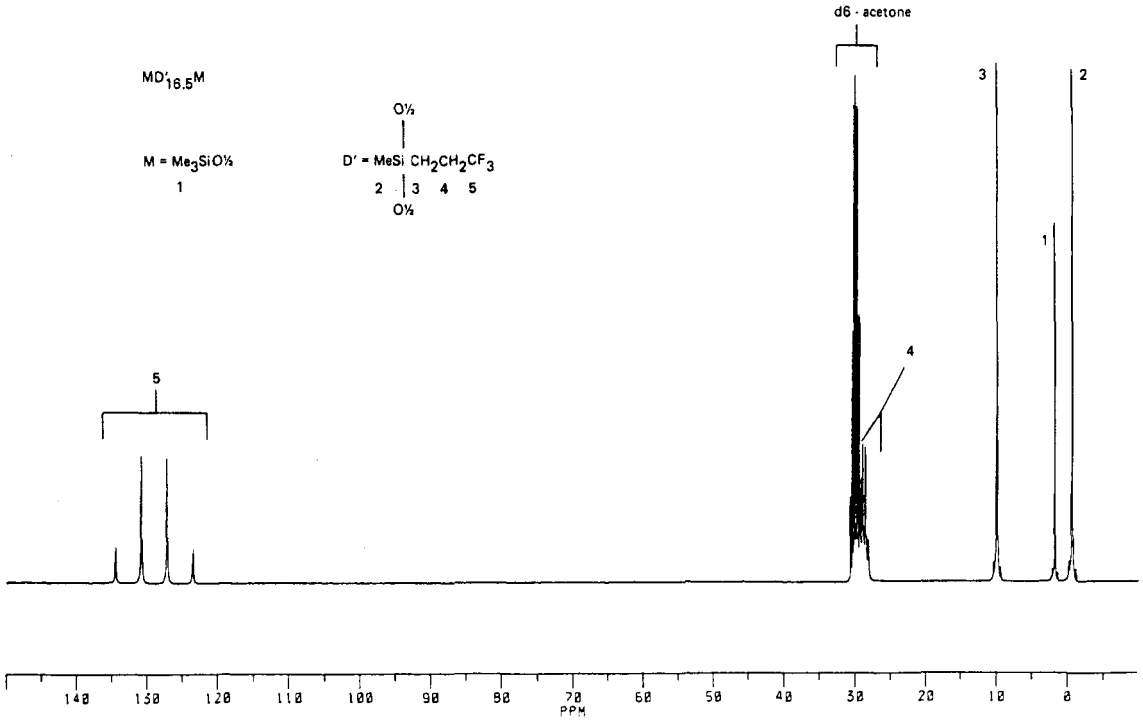


**Figure 4.** $^{13}C$ NMR spectrum of the polysiloxane A1.

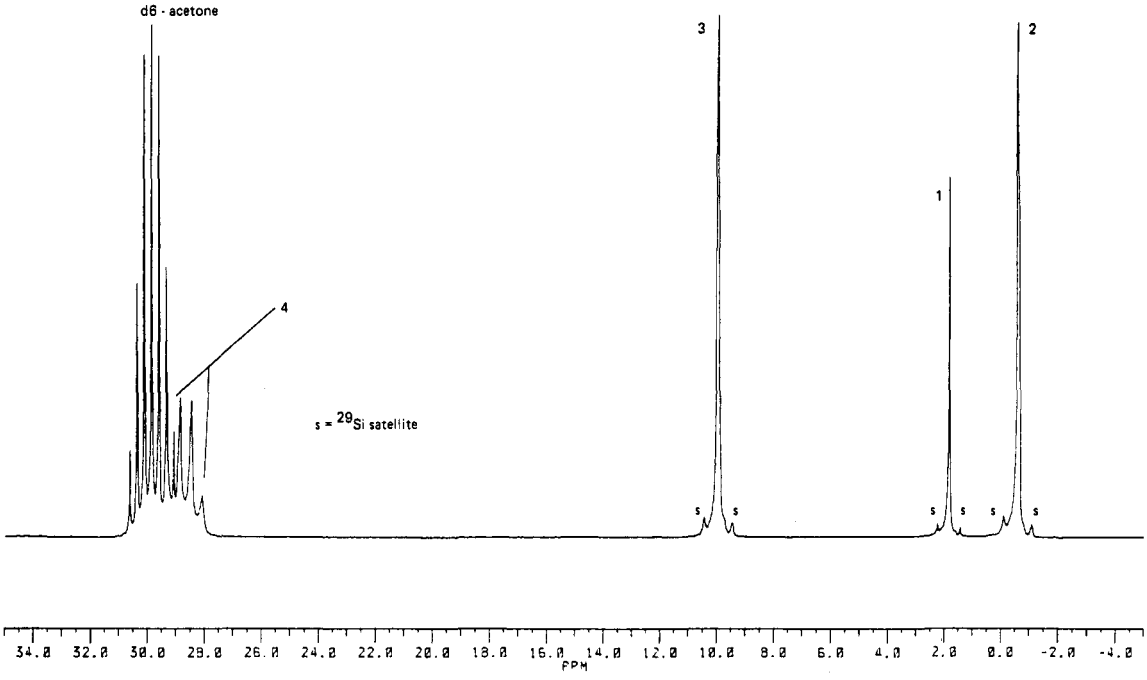


**Figure 5.** Low-frequency region of the $^{13}C$ NMR spectrum of A1 (see Figure 4 for structure).

It will noted that a number of resonances are observed for each triad grouping; there are two reasons for this. First, silicon chemical shift sensitivity extends beyond the triad level (i.e., pentad and heptad structures also need to be considered). Second, the asymmetry of the $D^1$ unit will induce further splittings since (neighboring) $D^1$ units can assume either *d* or *l* configurations. However, in the current analysis neither of these effects need to be considered.

The observed abundances of the six triad groups can now be used to establish conformity to a statistical model, which then enables the comprehensive description of the polymer microstructure. Full details of the statistical treatment applied here are given in the Appendix, with further information available from ref 5. For the purposes of this discussion, only a brief summary of the treatment need be given. For convenience, we will adopt a notation normally used in polymer analysis, such that D units will be designated by 0 and $D^1$ units by 1. Hence, the trial $DD^1D$ is described by 010, and so on.

The Bernoullian statistical model describes a purely random polymerization process, whereby the probability of addition of a monomer unit, 0 or 1, does not depend upon the nature of the preceding monomer unit. The polymer microstructure can therefore be described solely in terms of two probabilities, $P_0$ and $P_1$, where $P_0$ represents the probability of addition of unit 0 and $P_1$ the probability of addition of unit 1. (In fact, only one probability is required for a complete description since $P_0 + P_1 = 1$.) The probabilities $P_0$ and $P_1$ thus ultimately

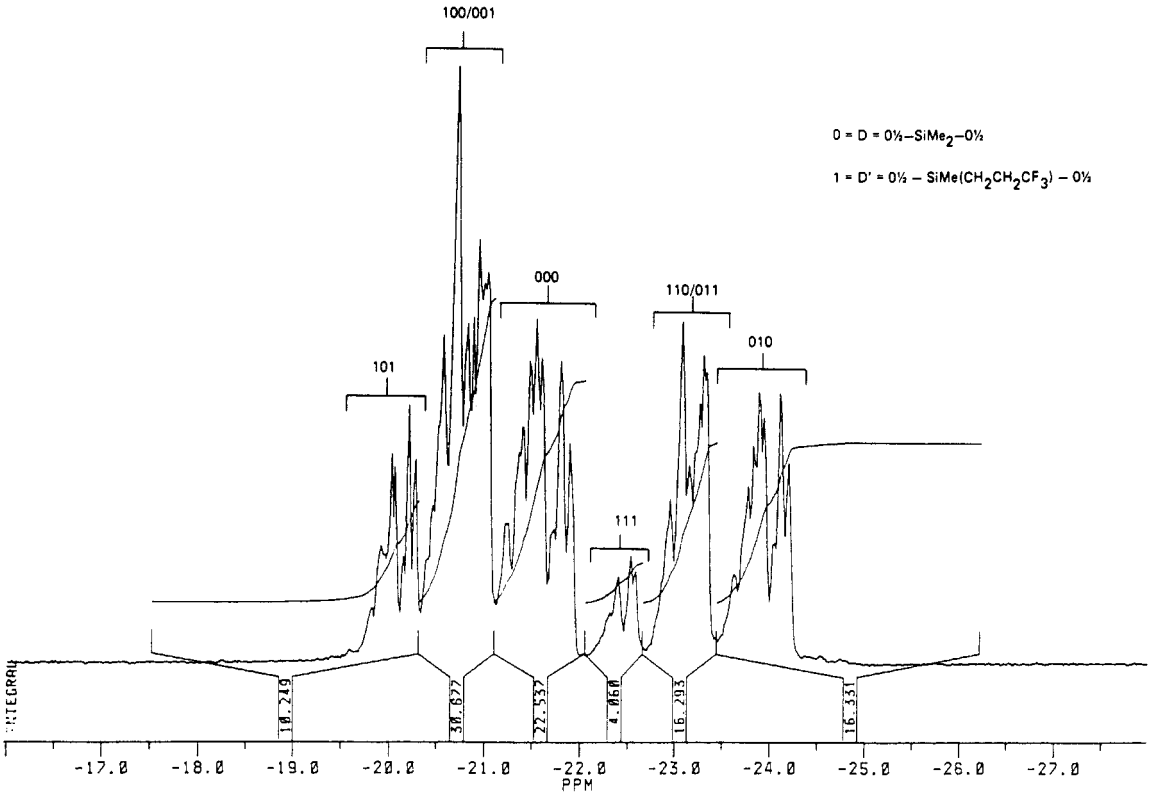


**Figure 6.** $^{29}Si$ NMR spectrum of B1 showing triad assignments.

**Table III**
**Observed and Calculated Triad Comonomer Distributions for the Polysiloxane Antifoam Agent B1**

| | | calcd distrib | |
|---|---|---|---|
| | | Bernoullian | first-order Markovian |
| triad[a] | obsd distrib | $P_0 = 0.635$ $P_1 = 0.365$ | $P_{10} = 0.67$ $P_{01} = 0.40$ |
| 000 | 0.225 | 0.256 | 0.225 |
| 001/100 | 0.308 | 0.294 | 0.301 |
| 101 | 0.102 | 0.085 | 0.100 |
| 010 | 0.163 | 0.147 | 0.168 |
| 001/110 | 0.162 | 0.169 | 0.165 |
| 111 | 0.040 | 0.049 | 0.041 |

[a] 0 = D = $O_{1/2}SiMe_2O_{1/2}$; 1 = $D^1$ = $O_{1/2}SiMe(CH_2CH_2CF_3)O_{1/2}$.

**Table IV**
**Composition of Antifoam Agent B1**

polysiloxane component
0 = D = $O_{1/2}SiMe_2O_{1/2}$
1 = $D^1$ = $O_{1/2}SiMe(CH_2CH_2CF_3)O_{1/2}$
monomer addition probabilities
$P_{10} = 0.67$ $P_{00} = 0.33$
$P_{01} = 0.40$ $P_{11} = 0.60$
mole fraction of D = $P_{10}/(P_{10} + P_{01}) = 0.63$
mole fraction of $D^1$ = $P_{01}/(P_{10} + P_{01}) = 0.37$
number-average sequence length of D = $1/P_{01} = 2.5$
number-average sequence length of $D^1$ = $1/P_{10} = 1.5$
$P_{10} > P_{11}$, $P_{01} > P_{00}$ → tendency toward alternating copolymer
cosolvent components
major: diisobutyl ketone (2,6-dimethylheptan-3-one)
minor: unidentified ketone, possibly $C_9$

correspond to the 0 and 1 mole fractions observed for the copolymers. For B1, $P_0$ and $P_1$ are readily established from the abundances of 0-centered triads (63.5%) and 1-centered triads (36.5%), respectively (see Table III). To check for conformity of B1 to the Bernoullian model, the mole fractions of the six triad groupings have been calculated (e.g., the mole fraction of 101 is given by $P_1^2P_0$); these are compared with the experimental values in Table IV. It is obvious from the results that B1 does not conform to the Bernoullian statistical model. We have therefore invoked a second statistical model commonly used for copolymer analysis.

In the first-order Markovian model, the probability of monomer addition depends upon the immediately preceding event. Thus, the probability of addition of a monomer unit, 0 or 1, depends upon the nature of the preceding unit. Four probabilities arise from the analysis: $P_{00}$, $P_{01}$, $P_{10}$, and $P_{11}$, where $P_{00}$ is the probability of addition of 0 to 0, $P_{01}$ is the probability of addition of 1 to 0, and so on. For B1, values of $P_{01}$ and $P_{10}$ have been established from our experimental data and have been used to calculate the mole fractions of the six triad groupings (see Appendix for details). Comparison of these data with observed triad abundances (see Table IV) clearly indicates that B1 conforms to the first-order Markovian model.

Using $P_{01}$ and $P_{10}$, we have determined the mole fractions of 0- and 1-type monomer, values for $P_{00}$ and $P_{11}$, and number-average sequence lengths for the B1 antifoam agent. An important conclusion from the statistical study is that an opposite sequence of monomer additions is favored over a like sequence of additions; that is, $P_{01} > P_{00}$ and $P_{10} > P_{11}$. In other words, the polysiloxane tends toward an alternating copolymer rather than a "blocky" copolymer.

**3.4. Characterization of Antifoam Agents B2 and B3. B2.** The silicon-29 NMR spectrum is shown in Figures 7 (full spectrum) and 8 (low-frequency region only). Comparison with our previous results indicates that the sample comprises a mixture of two polysiloxane components: one is essentially identical with the copolymer found in B1 (e.g., cf. Figures 6 and 8), while the other is very similar to the A1 homopolymer. Our carbon-13 NMR results lend full support to this formulation and also indicate the presence of the same cosolvents found in B1 (i.e., diisobutyl ketone and an unidentified $C_9$ ketone). From these results, we have calculated the ratio of copolymer to homopolymer as 70%: 30% by weight. In addition, we have estimated that the overall polymer concentration in

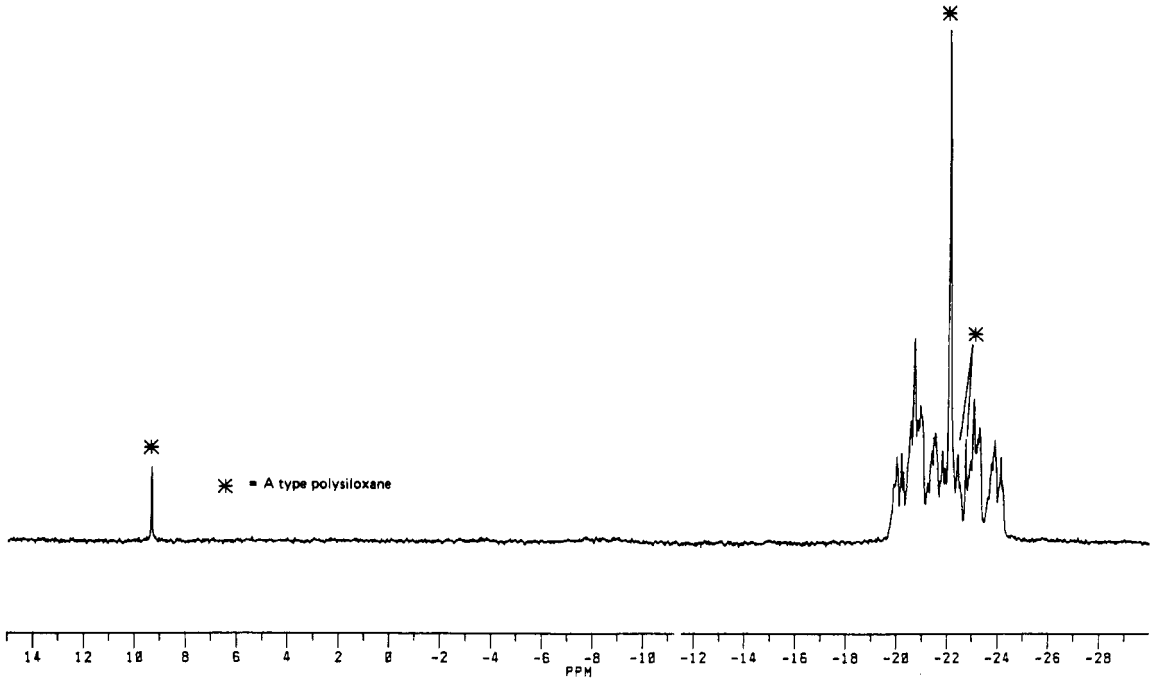


**Figure 7.** $^{29}Si$ NMR spectrum of B2.

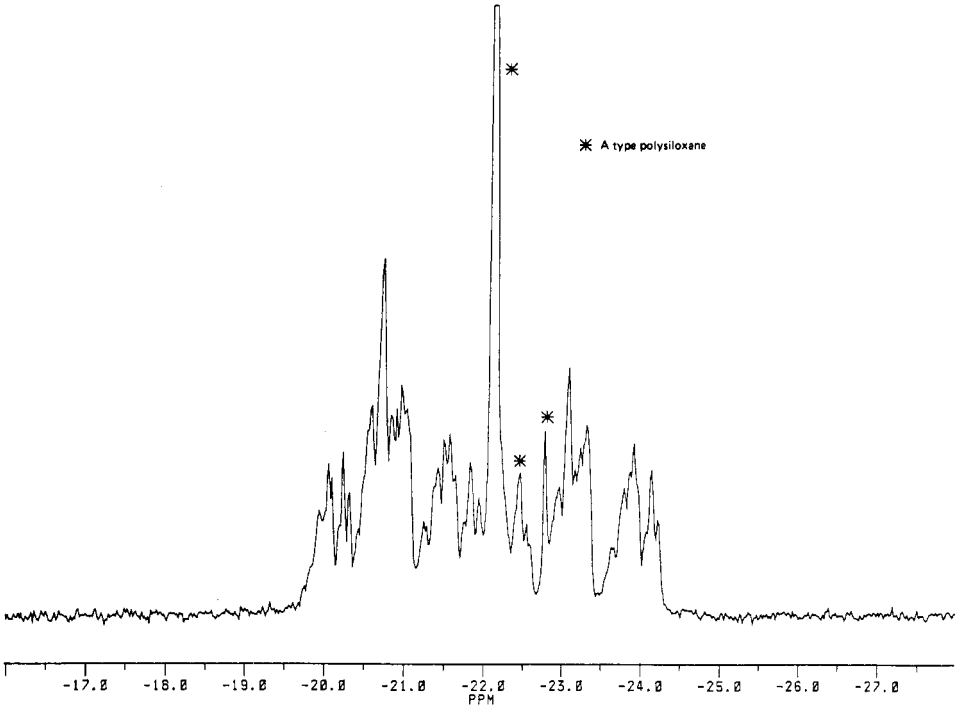


**Figure 8.** Low-frequency region of the $^{29}Si$ NMR spectrum of B2.

the sample is only 5% w/w; i.e., the sample comprises 95% w/w of cosolvent (this is in contrast to B1 where the polysiloxane concentration is approximately 50% w/w).

**B3.** The silicon-29 NMR spectrum of B3 is shown in Figure 9. The complexity of the spectrum again indicates that the polysiloxane is a (random) copolymer. Analysis of the carbon-13 NMR spectrum of this sample (not illustrated) reveals that the chain units present are the same as those observed in B1, namely, D = $O_{1/2}SiMe_2O_{1/2}$ and $D^1 = O_{1/2}SiMe(CH_2CH_2CF_3)O_{1/2}$. However, in comparison to B1, this sample has a much lower molecular weight since signals indicative of end-chain units M are clearly visible in both the $^{13}C$ and $^{29}Si$ spectra (see Figure 9). This presents a problem when attempting detailed analysis of the silicon-29 spectrum since the region due to $D/D^1$ units will contain significant contributions from $D/D^1$ units close to the ends of the polysiloxane chain. For this reason, we have not performed detailed microstructure analysis on B3.

However, it is still possible to calculate the ratio of D to $D^1$ units (1:1) and, in addition, the average chain length of the copolymer by ratioing $D/D^1$ intensity against M intensity. The average chain composition determined in this way is $MD_{12.5}D^1_{12.5}M$, which gives an average molecular weight of about 3000. From the carbon-13 NMR analysis, the major cosolvents present have been identified as 1,2,4-trimethylbenzene and methyl isobutyl ketone (4-methylpentan-2-one). Other minor solvent components were also detected (mainly methyl-substituted benzenes). Moreover, the cosolvents account for approximately 60%

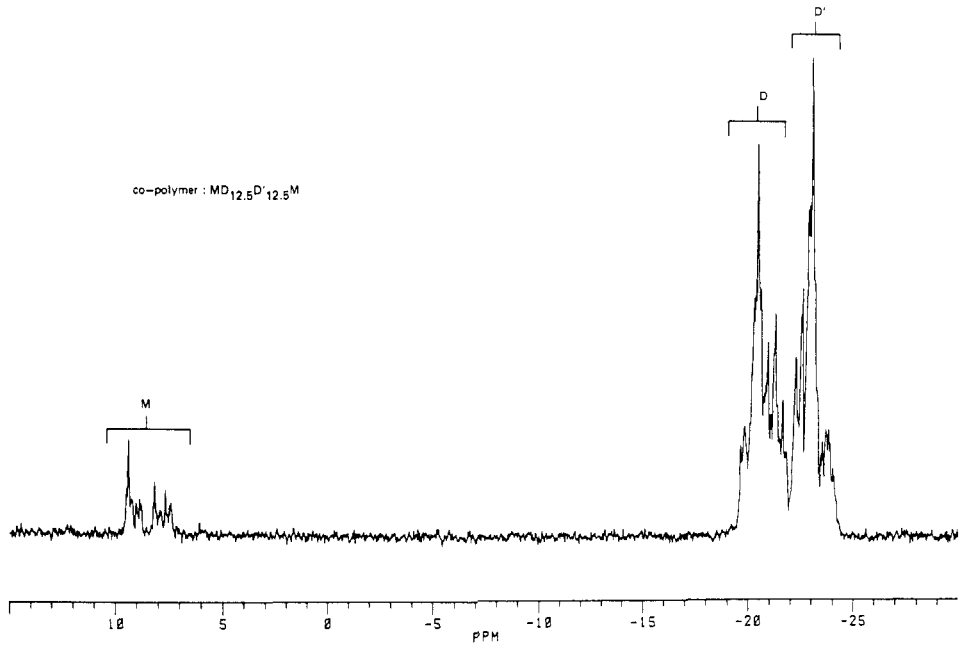


**Figure 9.** $^{29}Si$ NMR spectrum of B3.

by weight of the total sample.

## 4. Conclusions

Due consideration of the properties of the silicon-29 nucleus enables selection of conditions appropriate for quantitative NMR analysis.

A combination of carbon-13 and silicon-29 NMR spectroscopy leads to full structural characterization of polysiloxane antifoam agents. In most cases, this includes determination of average molecular weights.

For copolymers, statistical analysis of observed triads abundances yields a detailed description of polymer microstructure.

## Appendix

**Statistical Analysis of Copolymer Microstructure.** The use of two statistical models to describe the microstructure of a copolymer is discussed here. Further details of these models can be found in ref 5. In this work, the models have been applied to a polysiloxane copolymer, but they are equally applicable to other systems.

**Bernoullian Statistical Analysis.** The Bernoullian model describes a random distribution of comonomer units where the probability of a monomer addition is independent of the outcome of any previous addition. Consequently, only two addition probabilities need to be defined, $P_0$ and $P_1$, which represent the probabilities of 0 and 1 additives, respectively. Since only 0 or 1 addition can occur

$$P_0 + P_1 = 1 \tag{A1}$$

(note, therefore, that only one independent variable is required for Bernoullian analysis). The six triad abundances in a copolymer are then given by the following set of equations:

$$[000] = P_0^3 \tag{A2}$$

$$[001] + [100] = 2P_0^2P_1 \tag{A3}$$

$$[101] = P_0P_1^2 \tag{A4}$$

$$[010] = P_0^2P_1 \tag{A5}$$

$$[011] + [110] = 2P_0P_1^2 \tag{A6}$$

$$[111] = P_1^3 \tag{A7}$$

Ultimately, $P_0$ and $P_1$ correspond to the 0 and 1 mole fractions and can normally be determined directly from an NMR spectrum (e.g., as was the case for B1). A Bernoullian fit is usually then established after a comparison of an observed trial distribution with that calculated with eq A2–A7. (Note B1 did not conform to a Bernoullian model—see Table IV.) If a Bernoullian fit is successful, then the number-average sequence lengths of successive 0 or 1 additions are as follows:

$$n_0 = 1/P_1 \tag{A8}$$

$$n_1 = 1/P_0 \tag{A9}$$

**First-Order Markovian Statistical Analysis.** A first-order Markov system has addition probabilities that depend upon the nature of the immediately preceding monomer unit. Thus, four addition or transition probabilities need to be defined, $P_{00}$, $P_{01}$, $P_{10}$, and $P_{11}$, where $P_{00}$ represents the probability of 0 addition to 0, $P_{01}$ represents 1 addition to 0, and so on. The relationship between these four transition probabilities is as follows:

$$P_{00} + P_{01} = 1 \tag{A10}$$

$$P_{11} + P_{10} = 1 \tag{A11}$$

because a chain ending in 0 can only add 0 or 1, and likewise, a chain ending in 1 can also only add 0 or 1 (note, therefore, two independent variables are required to define a first-order Markov process ).

It can be shown that the triad distributions are given as follows:

$$[000] = P_{10}(1 - P_{01})^2/(P_{01} + P_{10}) \tag{A12}$$

$$[001] + [100] = 2P_{01}P_{10}(1 - P_{01})/(P_{01} + P_{10}) \tag{A13}$$

$$[101] = P_{01}^2P_{10}/(P_{01} + P_{10}) \tag{A14}$$

$$[010] = P_{01}P_{10}^2/(P_{01} + P_{10}) \tag{A15}$$

$$[011] + [110] = 2P_{01}P_{10}(1 - P_{10})/(P_{01} + P_{10}) \tag{A16}$$

$$[111] = P_{01}(1 - P_{10})^2/(P_{01} + P_{10}) \tag{A17}$$

Dividing eq A12 by eq A13, for example, leads to an expression for $P_{01}$

$$P_{01} = \frac{1}{\left[2\frac{[000]}{[001] + [100]} + 1\right]} \quad \text{(A18)}$$

A similar expression for $P_{10}$ can also be obtained. Thus, from observed triad abundances, values for $P_{01}$ and $P_{10}$ can be calculated. Conformity to the first-order Markovian model can then be determined after a comparison of observed triad distribution with that calculated from eq A12–A17 (e.g., see results for B1, Table III).

If a successful fit is obtained, then mole fractions of 0 to 1 are given by eq A19 and A20, respectively:

$$[0] = \frac{P_{10}}{P_{01} + P_{10}} \quad \text{(A19)}$$

$$[1] = \frac{P_{01}}{P_{01} + P_{10}} \quad \text{(A20)}$$

Number-average sequence lengths for 0 and 1 are given by the following expressions:

$$n_0 = 1/P_{01} \quad \text{(A21)}$$

$$n_1 = 1/P_{10} \quad \text{(A22)}$$

Finally the relationships between the probabilities $P_{00}$ and $P_{10}$ and $P_{01}$ and $P_{11}$ prove to be particularly useful in describing the polymer microstructure. There are three possible cases.

Case 1: $P_{10} > P_{00}$, $P_{01} > P_{11}$

For this case, an opposite sequence of monomer additions is favored over a like sequence of additions; i.e., there is a tendency toward an alternating copolymer.

Case 2: $P_{10} < P_{00}$, $P_{01} < P_{11}$

Here a like sequence of monomer additions is favored, indicating that there is a tendency toward formation of a "blocky" copolymer.

Case 3: $P_{10} = P_{00}$, $P_{01} = P_{11}$

For this case, monomer addition probabilities do not depend upon the nature of the preceding monomer unit; i.e., they reduce to a Bernoullian system, which describes a purely random comonomer distribution. Thus, any Bernoullian system can actually be described as a special case of the first-order Markov system.

## References and Notes

(1) Harris, R. K.; Mann, B. E. *NMR and the Periodic Table*; Academic Press: London, 1978; ISBN, 0-12-327650-0.
(2) Harris, R. K.; Kimber, B. J. *Appl. Spectrosc. Rev.* **1975**, *10*, 117.
(3) Harris, R. K.; Kimber, B. J. *J. Chem. Soc., Chem. Commun.* **1974**, 559.
(4) Jansken, H.; Engelhardt, G.; Kriegsmann, H.; Keller, F. *Plaste Kautsch.* **1979**, *26*, 612.
(5) Randall, J. C. *Polymer Sequence Determination—Carbon-13 NMR Method*; Academic Press: New York, 1977; ISBN, 0-12-578050-8.

# Organotin-Mediated Synthesis of Macrocyclic Tetraesters. A Combined $^1$H NMR Spectroscopy, Gel Permeation Chromatography, and Fast Atom Bombardment Mass Spectrometry Approach to Complete Product Analysis[1]

**Luigi Mandolini***

*Centro CNR di Studio sui Meccanismi di Reazione, Dipartimento di Chimica, Università "La Sapienza", 00185 Roma, Italy*

**Giorgio Montaudo* and Emilio Scamporrino**

*Dipartimento di Scienze Chimiche dell'Università di Catania, 95125 Catania, Italy*

**Stefano Roelens***

*Centro CNR di Studio sulla Chimica e la Struttura dei Composti Eterociclici e loro applicazioni, 50121 Firenze, Italy*

**Daniele Vitalini**

*Istituto per la Chimica e la Tecnologia dei Materiali Polimerici, CNR, 95125 Catania, Italy.*
*Received August 30, 1988*

ABSTRACT: A complete product analysis of the reaction of 2,2-di-*n*-butyl-1,3,2-dioxastannolane with a series of diacyl dichlorides in the organotin-mediated synthesis of macrocyclic polyesters has been performed by combined $^1$H NMR, GPC, and FABMS techniques. The experimental results provide unambiguous evidence that the product mixtures are well-behaved equilibrium distributions of cyclic oligomers, in which the absence of anomalous abundance for any of the macrocyclic products points to the lack of selectivity features that might be ascribed to a tin-template effect, as suggested by other authors.

## Introduction

The reaction of cyclic stannoxanes such as 2,2-di-*n*-butyl-1,3,2-dioxastannolane (**1**) with diacyl dichlorides (**2**) has been reported by Shanzer and co-workers[2] as a convenient, one-pot procedure for the selective synthesis of macrocyclic dimeric tetraesters (**3**, $n = 2$) of reflection symmetry (eq 1). The reaction was supposed to take advantage of the ability of tin to act as a covalent template in the dimeric structure of **1** in solution. Consistently, exclusive formation of the dimeric tetraesters **3**, $n = 2$, and other remarkable selectivity features were believed to arise from the ability of the tin template to assemble the reacting molecules in

0024-9297/89/2222-3275$01.50/0 